CONTACT BUCKLING AND POST-BUCKLING OF DELAMINATED PLATES

Herzl Chai[1]

Summary

A combined experimental/analytic approach is employed to gain insight into the mechanics of contact between flexible beam or plate elements and a stiff substrate under compression loading. The outward displacement of the buckled structure is determined in real-time via the shadow Moire technique. The lateral constraints lead to a sequential plate snapping process that arise from secondary buckling within the buckle(s) or at contact zone(s) in the plate. The critical load for mode transition is evaluated systematically as a function of the confinement gap, h, the plate aspect ratio, R, and other system parameters. The results generally exhibit significant scatter that is attributed to the inherent asymmetry of the deformation pattern in such systems. A large-deformation finite element analysis incorporating frictional contact algorithm is used to model the post buckling deformation. The deformation patterns as well as the critical loads predicted from this analysis generally agree well with the experimental results. A simple analytic expression, based on the linear theory of beam-columns, is developed for the critical loads. The experimental data are found to be well contained by the lower and upper bounds from this analysis once the plate surface begin to interact with both of the confining planes. In addition to providing basic insight, the results of this work may serve as a basis for multi laminate design possessing unique mechanical response and superior energy absorption capability.

Introduction

The mechanics of contact between flexible beam or plate elements and a stiff substrate under compression environment is of interest in a variety of engineering applications, including deep drilling (Wu and Juvkam-Wold, 1995), near-surface delamination (Chai, 1981, Jones et al, 1985, Whitcomb, 1988, Chai, 1990, Nilsson and Giannakopoulos, 1995, Shahwan and Waas, 1997, and Sekine et al, 2000), sheet metal forming processes (e.g. Gupta et al 1999, Kim et al, 2000) and encased plate sections in civil engineering structures (Wright, 1995).

In this work, a systematic study is carried out to elucidate the effects of plate aspect ratio, the gap between the constraining walls and the load level on the plate response. Clamp type boundary support is assumed in order to simulate thin-film delamination problems. The outward plate deformation is observed in real-time via the shadow Moire technique. A large-strain finite element analysis incorporating a frictional contact algorithm is used to model the plate behavior.

1. Department of Solid Mechanics, Materials and Systems, Faculty of Engineering, Tel Aviv University

Results

Fig. 1 shows a mid section of the bi-laterally constrained plate. As shown, the plate is constrained by two rigid walls forming a gap *h*. The plate is clamped on all four edges while subjected to a uniform vertical displacement at its upper edge. Fig. 2 and 3 exemplify the deformation sequence due to axial compression in a unilaterally and a bilaterally constrained polycarbonate plates confined between glass surfaces. The normalized edge displacement in this illustration is given as

$$K = \frac{12(1-v^2)b^2}{\pi^2 t^2} \frac{\Delta}{a}$$

where *t*, *b* and *a* are the thickness, width and length of the plate, in that order, and Δ denote the axial displacement applied to the specimen edge. Fig. 2 shows that plate snapping is motivated from local buckling at the edges of the buckle. In contrast, buckling mode transition in the bilaterally constrained plate occurs as a result of local buckling from contacting segments in the plate. One also observes in this case that the deformation resembles a one-dimensional pattern once several buckles are generated. It is interesting to note that other plate snapping phenomenon was also observed by Falzon and Steven, 1997, for unconstrained, hat-stiffened composite panels.

A one dimensional, beam-column structure was analysis was developed to account for the mode transition phenomenon in the bi-laterally constrained plate. The sequence of deformation in the column is shown in Fig. 4. Mode transition occurs due to buckling of the longest of the contact segments. The analysis shows that one may vary the individual lengths of the contacting segments while keeping their total length without affecting the strain energy in the column. This implies a degree of statistical variation in the mode transition load. The latter can be bounded, however. As shown in Fig. 5 for the case of two buckles, the lowest mode transition load occurs if all the flattened segments are assigned to a single segment. On the other hand, the highest snapping load would be realized if all the contacting segments are of equal length. Using the technical theory of beams and plates, the following bounds for the buckling mode transition are arrived (Chai, 1998, 2000, 2002),

$$(1+2n)[1+2n+\frac{9n(h/t)^2}{2\pi^2}] \leq \overline{\Delta}_n \leq (1+4n)[1+4n+\frac{9n(h/t)^2}{2\pi^2}],$$

$$\overline{\Delta} \equiv \frac{3(\Delta/a)}{\pi^2(t/a)^2}$$

where $\overline{\Delta}_n$ is the normalized axial displacement at the transition from *n* to *n + 1* buckles, and the expressions on the left and right sides of this equation correspond to the lower and upper bounds, respectively. Fig. 6 shows that this

relation bounds well the experimental data for the bilaterally constrained plate once several buckles occur.

References

H. Chai. (1981): "The growth of impact damage in compressively loaded laminates". Ph.D. thesis, Caltech.

Chai, H. (1990): "Three-dimensional analysis of thin-film debonding". *International Journal of Fracture*, Vol. 46, pp. 237-256.

Chai, H. (1998): "The post-buckling behavior of a bilaterally constrained column". *Journal of the Mechanics and Physics of Solids,* Vol. 46, pp. 1155-1181.

Chai, H. (2000): "Contact buckling and post-buckling behavior of thin rectangular plates". *Journal of the Mechanics and Physics of Solids,* Vol. 49, pp. 203-230.

Chai, H. (2002): "On the post-buckling behavior of bilaterally constrained plates". *International Journal of Solids and Structures* Vol. 39, pp. 2911-2926.

Falzon, B.G. and Steven, G.P. (1997): "Buckling mode transition in hat-stiffened composite panels loaded in uniaxial compression". *Composite Structures* Vol. 37, pp. 253-267.

Gupta, N.K., Easwara Prasad and Gupta, S.K. (1999): "Axial compression of metallic spherical shells between rigid plates". *Thin-Walled Structures* Vol. 34, pp. 21-41.

Jones, R., Broughton, W., Mousley, R.F. and Potter, R.T., 1985. Compression failure of damaged graphite epoxy laminates. In Composite Structures, Elsevier Publishers, England.

Kim, J.B., Yoon J.W. and Yang D.Y. (2000): "Wrinkling initiation and growth in modified Yoshida buckling test: Finite Element analysis and experimental comparison". *International Journal of Mechanical Sciences,* Vol. 42, pp.1683-1714.

Nilsson, K.L. and Giannakopoulos, A.E. (1995): "A finite element analysis of configurational stability and finite growth of buckling driven delamination". *Journal of the Mechanics and Physics of Solids*, Vol. 43, pp. 1983-2021.

Sekine, H., NU, H. and Kouchakzadeh, M. A. (2000): "Buckling analysis of elliptically delaminated composite laminates with consideration of partial closure of delamination". *Journal of Composite Materials,* Vol. 34, pp. 551-573.

Shahwan, K.W. and Waas, A.M. (1997): "Non-self-similar decohision along a finite interface of unilaterally constrained delaminations". *Proceedings of the Royal Society of London, Vol.* A 453, pp. 515-550.

Whitcomb J.D. "Instability-related delamination growth of embedded and edge delamination", NASA Technical Memorandum 100655, Aug. 1988.

Wright H.D. (1995): "Local stability of filled and encased steel sections". *Journal of Structural Engineering,* Vol. 12, pp. 1382-1388.

Wu., J. and Juvkam-Wold, H., C. (1995): "Buckling and lockup of tubulars in inclined wellbores". *Journal of Applied Mechanics,* Vol. 117, pp. 208-213.
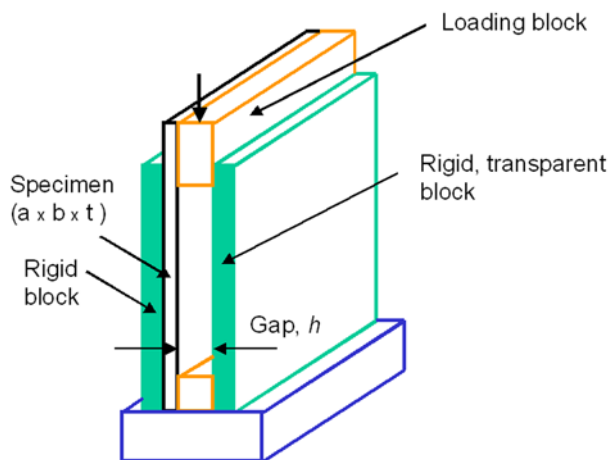
Fig. 1. Bi-laterally constrained column or plate;sectional view

I. K=25.3   II. K=68.4   III. K=84.4   IV. K=86.4

I. K=25.3   II. K=68.4   III. K=84.4   IV. K=86.4
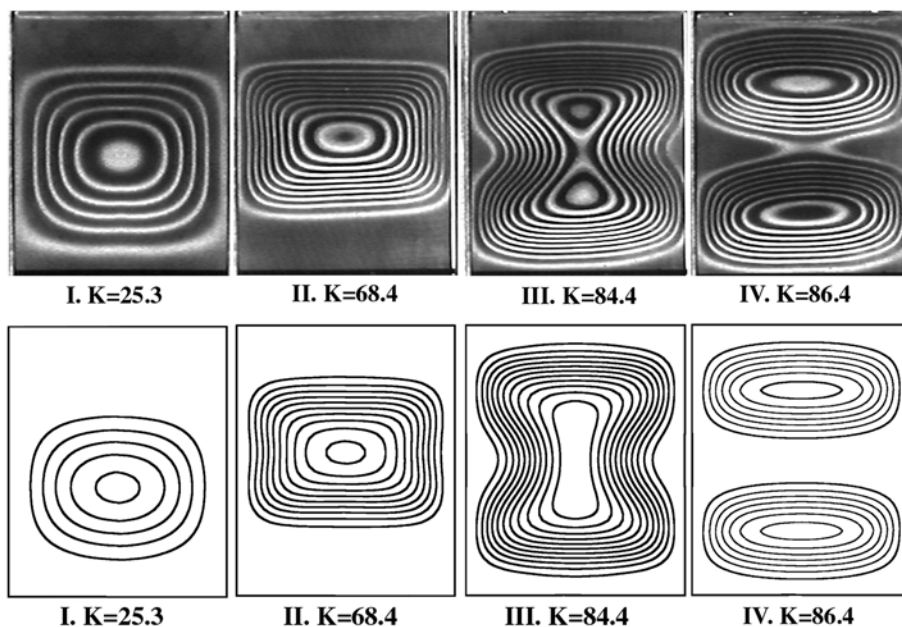
Fig. 2. Outward Moire displacement contours at increasing normalized axial displacement for unilaterally constrained plate ($h \rightarrow \infty$), $t = 0.7$ mm, $b = 76.2$ mm, $R = 1.2$, fringe constant, f, is 0.3mm; upper sequence corresponds to

experiments, lower sequence is FEM prediction based on the same load levels as above.

I. K=10.7   II. K=32.1   III. K=91.5   IV. K=92   V. K=193   VI. K=297
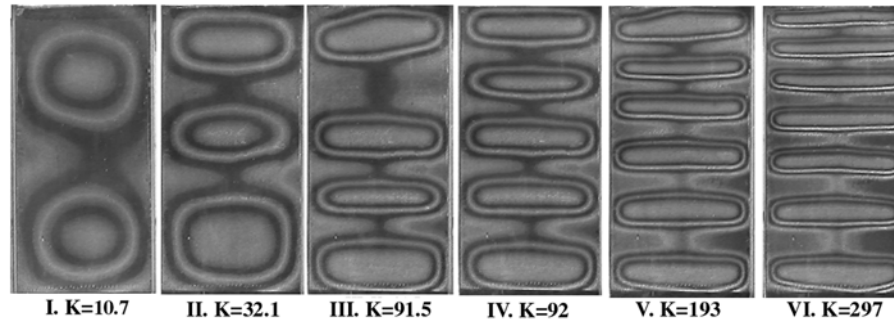
Fig. 3. Outward Moire displacement contours for bilaterally constrained plate, t = 0.5 mm, b = 76.2 mm, R = 2, h = 0.5 mm, f = 0.3 mm. Each of the prints corresponds to just after the completion of buckling mode transition.
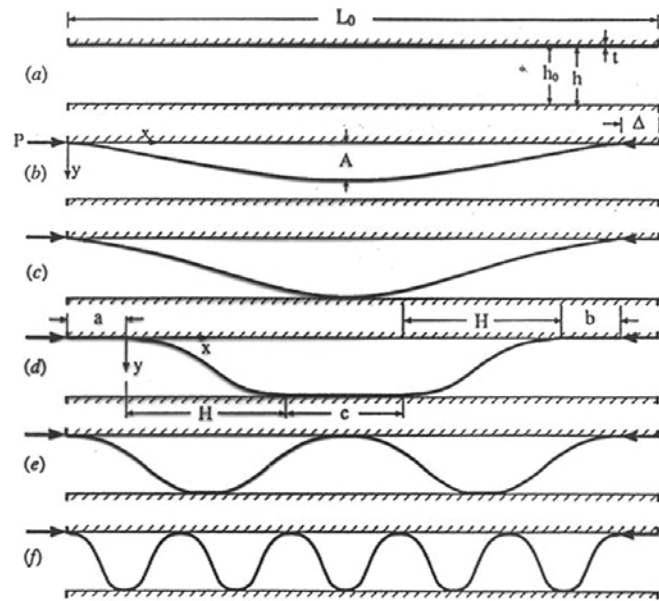
Fig. 4. The deformation sequence of a bi-axially constrained column
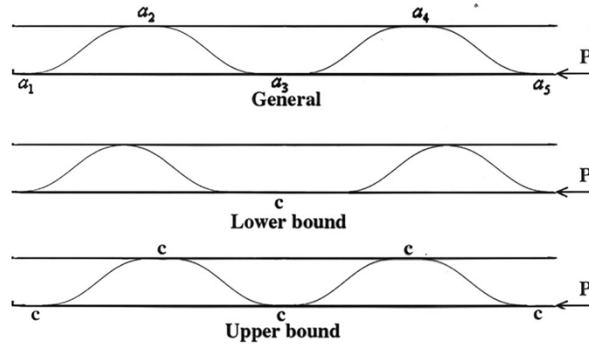
Fig. 5. Illustration of extreme configurations for bi-laterally constrained column for the case of two buckles
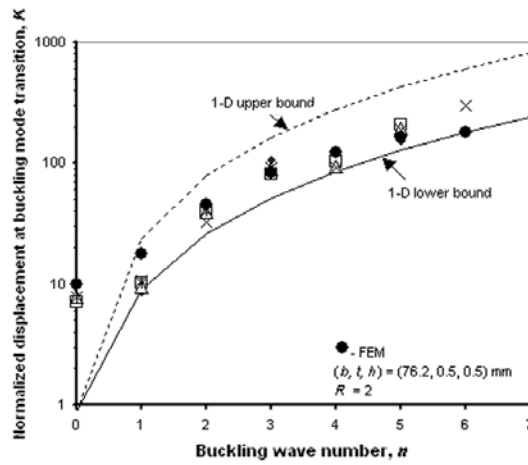
Fig. 6. End displacement vs. buckling wave number for the bilaterally constrained plate shown in Fig. 3.